THE JOURNAL OF PHYSICAL CHEMISTRY B

Article

pubs.acs.org/JPCB

Energy Transfer and Trapping in Red-Chlorophyll-Free Photosystem I from *Synechococcus* WH 7803

Ivo H.M. van Stokkum,[†] Thibaut E. Desquilbet,[‡] Chantal D. van der Weij-de Wit,[†] Joris J. Snellenburg,[†] Rienk van Grondelle,[†] Jean-Claude Thomas,[§] Jan P. Dekker,*[,†] and Bruno Robert[†,‡]

[†]Institute for Lasers, Life and Biophotonics, Faculty of Sciences, VU University Amsterdam, De Boelelaan 1081, 1081 HV Amsterdam

[‡]CEA, Institut de Biologie et de Technologies de Saclay, and CNRS, 91191 Gif/Yvette Cedex France

[§]Biologie Moléculaire des Organismes Photosynthétiques, Unité Mixte de Recherche 8186, Ecole Normale Supérieure, 46 rue d'Ulm, 75230 Paris Cedex 05, France

Supporting Information

ABSTRACT: We report for the first time steady-state and time-resolved emission properties of photosystem I (PSI) complexes isolated from the cyanobacterial strain *Synechococcus* WH 7803. The PSI complexes from this strain display an extremely small fluorescence emission yield at 77 K, which we attribute to the absence of so-called red antenna chlorophylls, chlorophylls with absorption maxima at wavelengths longer than those of the primary electron donor P700. Emission measurements at room temperature with picosecond time resolution resulted in two main decay components with lifetimes of about 7.5 and 18 ps and spectra peaking at about 685 nm. Especially in the red flanks, these spectra show consistent differences, which means that earlier proposed models for the primary charge separation reactions based on ultrafast (~1 ps) excitation equilibration processes cannot describe the data. We show target analyses of a number of alternative models and conclude that a simple model (Ant2)* ↔ (Ant1/RC)* → RP2 can explain the time-resolved emission data very well. In this model, (Ant2)* represents chlorophylls that spectrally equilibrate in about 7.5 ps and in which RP2 represents the "final" radical pair $P700^+A_0^-$. Adding an equilibrium (Ant1/RC)* ↔ RP1, in which RP1 represents an "intermediate" radical pair $A^+A_0^-$, resulted in the same fit quality. We show that the simple model without RP1 can easily be extended to PSI complexes from cyanobacteria with one or more pools of red antenna chlorophylls and also that the model provides a straightforward explanation of steady-state emission properties observed at cryogenic temperatures.

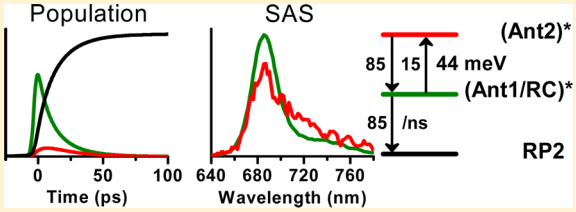

INTRODUCTION

Photosystem I (PSI) is a membrane-bound pigment−protein complex essential to photosynthesis; see, for example, ref 1. It uses light energy to transport electrons from reduced plastocyanin or cytochrome c_6 to soluble ferredoxin during the first steps of oxygenic photosynthesis, thus generating chemical species with a redox potential low enough to ultimately reduce $NADP^+$ to NADPH. To achieve this function, PSI binds many light-harvesting pigments (chlorophyll (Chl) and carotenoid molecules) that efficiently absorb the solar photons and transfer the resulting excitation energy to the photochemical reaction center (RC), where charge separation and subsequent electron-transfer reactions takes place.

The understanding of the primary charge separation and electron-transfer reactions is hampered by the presence of Chl molecules possessing absorption transitions at wavelengths longer than the primary electron donor, P700. Depending on the organism, various spectral forms of the so-called "red Chls" were observed, both in the core antenna and (in green plants and algae) in the peripheral antenna, emitting at wavelengths as long as 720−760 nm; see, for example, refs 2−4. These red Chls can be characterized by their steady-state emission properties at cryogenic temperatures, where they are easily observed in view of their long fluorescence lifetimes. The overall trapping kinetics in PSI strongly depends on the presence of these spectral forms, which compete with the primary electron donor P700 and make a straightforward interpretation of the trapping data complicated.

The trapping of excitation energy by charge separation has been estimated to occur in ~20−30 ps in PSI core particles from green plants, green algae like *Chlamydomonas reinhardtii*, and some cyanobacteria, whereas in PSI of cyanobacteria with additional red Chls and in native plant and algal PSI complexes with additional peripheral antenna subunits, longer trapping times were observed.[5−8] In the past decade, research on the primary charge separation processes in PSI was focused on those in PSI core complexes of *Chlamydomonas reinhardtii*[9−12] because these complexes were thought to have only a small number of red Chls and because it was possible in

Special Issue: Rienk van Grondelle Festschrift

Received: February 6, 2013
Revised: May 6, 2013
Published: July 8, 2013

   dx.doi.org/10.1021/jp401364a | J. Phys. Chem. B 2013, 117, 11176−11183

Chlamydomonas to generate mutants near the primary reactants with verifiable effects on the primary electron-transfer processes. In those complexes, the decay of the fluorescence at RT occurred predominantly in two phases with lifetimes of about 7−8 and 22−25 ps.[11,12] The first phase was attributed to the equilibration of the excitation energy between the antenna and the first radical pair state (most likely the state $A^+A_0^-$), and the second phase was attributed to the stabilization of the radical pair by electron transfer from P700 to A^+.[13] Although it was claimed by some authors that PSI core particles from *Chlamydomonas* did not contain any red Chl, low-temperature (77 K) emission spectra of PSI core complexes from *Chlamydomonas* revealed consistently a strong emission band referred to as F715; see, for example, refs 14 and 15, suggesting that these complexes do contain a small number of red Chls.

In this paper, we have studied for the first time PSI particles isolated from a cyanobacterial strain, *Synechococcus* WH 7803, that have a very low yield 77 K fluorescence emission spectrum (orders of magnitude smaller than observed for PSI complexes from other organisms). We suggest that PSI from *Synechococcus* WH 7803 does not contain any red Chl at all, in contrast to, for example, PSI cores from *Chlamydomonas reinhardtii*. By recording time-resolved fluorescence measurements at room temperature, followed by global and target analysis, we could obtain a comprehensive picture of the energy-transfer and charge separation processes in PSI in this and other cyanobacteria.

MATERIALS AND METHODS

Cell Culture and Growth Conditions. *Synechococcus* sp. strain WH 7803 (from the Woods Holes Oceanographic Institution, U.S.A.) was grown in an artificial seawater medium[16] at 20 °C with 10 μE m^{-2} s^{-1}. *Synechocystis* sp. strain PCC 6803 was grown axenically in a BG-11 medium[17] at 30 °C under continuous illumination provided by fluorescent white lamps, giving an intensity of 70 μE m^{-2} s^{-1}. Experimental cultures were continuously bubbled with sterile air.

Thylakoid Extraction and PSI Isolation. Thylakoid extraction was performed as described previously.[18] PSI was purified by sucrose density gradient centrifugation, as described previously.[19] Further experiments were performed on the lowest sucrose gradient band containing PSI trimers, which was verified by electron microscopy (E. J. Boekema, unpublished observations).

Absorption Spectra. The 4 K absorption measurements were performed on a Cary 5 spectrophotometer (Varian, Palo Alto, California, U.S.A.) equipped with a gas-flow helium cryostat (Air Liquide, Sassenage, France).

Fluorescence Emission Spectra. The 77 K fluorescence emission spectra were measured with a F-4500 Hitachi fluorescence spectrophotometer (Tokyo, Japan), with an excitation wavelength (half-bandwidth, 5 nm) at 440 nm. Fluorescence emission was recorded from 620 to 800 nm (half-bandwidth, 2.5 nm). Low-temperature fluorescence measurements (at 77 and 5 K) were performed on a Raman spectrometer (Jobin Yvon, Longjumeau, France) equipped with a front-illuminated, deep-depleted CCD detector (Jobin-Yvon). The Chl concentrations of different samples were made the same before the experiment by dilution with buffer.

Time-resolved fluorescence after 400 nm excitation was measured at the magic angle using a synchroscan streak camera system[20] at 111 wavelengths from 610 to 780 nm with an instrument response function (IRF) of 4.1 ps full width at half-maximum. During the streak experiment, the free Chl contribution increased slightly due to a small amount of damage to the sample and was much higher than that during the steady-state spectrum measurement.

All traces were globally analyzed to find the minimal number of lifetimes and decay-association spectra (DAS) needed for a satisfactory description of the data. Subsequently, we employed target analysis[21,22] using different kinetic schemes in combination with spectral assumptions[23,24] to resolve the minimal number of functional compartments. The basic model (see Figure 1) consists of two antenna compartments with natural

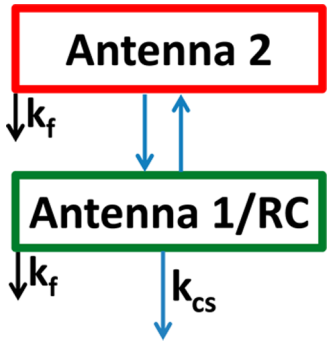

Figure 1. Functional compartmental model describing PSI dynamics at RT.

decay rates k_f, which are in equilibrium with each other. The antenna 1 compartment contains a RC from which charge separation can occur, and therefore, this compartment has an additional decay rate k_{cs}. The free-energy difference between the two compartments depends on the energy difference between the two emission maxima and on the relative number of pigments of the compartments ($k_BT\ln(N_1/N_2)$).

From the target analysis, we estimated species-associated spectra (SAS) and microscopic rate constants describing the kinetics. To enforce non-negative SAS, we employed a non-negative least-squares variable projection algorithm.[23] Even when we assumed that k_f was known (typically 1/(5 ns)), the model of Figure 1 contained three unknown microscopic rate constants. The two emissive compartments will yield only two lifetimes, which means that in order to estimate all rate constants, we require an additional constraint. Assuming that equal areas of the two SAS (i.e., equal oscillator strengths) provided us with this constraint[24] and enabled estimation of all unknown kinetic parameters. Thus, we resolved the equilibrium and determined the free-energy difference between the two states.

When a kinetic scheme contains a complete equilibrium between three compartments, 1 ⇄ 2 ⇄ 3 ⇄ 1, a detailed balance condition needs to be fulfilled. This constraint limits the number of free parameters of this 1−2−3 cycle to five.[25] This number can be reduced to three by assuming an equal area of all SAS, again allowing us to resolve all microscopic rate constants when three lifetimes can be estimated.

RESULTS

Steady-State Spectroscopy at Cryogenic Temperatures. The strain *Synechococcus* WH 7803 was chosen for this study after screening more than 100 strains in the collection of cyanobacteria of the Ecole Normale Supérieure, on the basis of their fluorescence properties at low temperature.

PSI particles were purified from this strain and characterized by their absorption and emission properties. A low-temperature (4 K) absorption spectrum of these isolated (trimeric) PSI particles is displayed in Figure 2, together with that of the

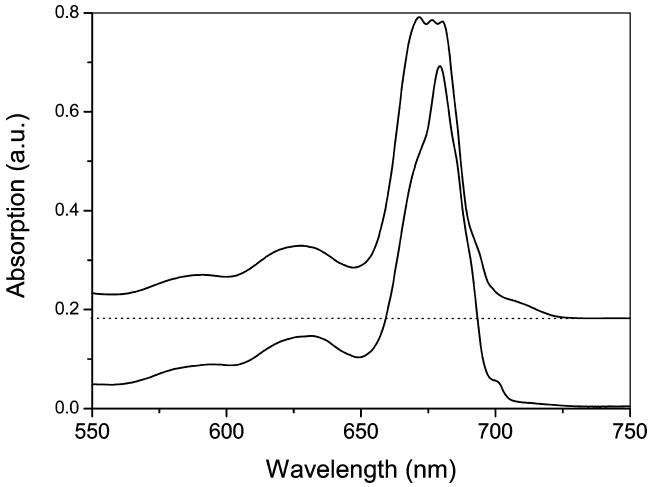

Figure 2. Absorption spectra (recorded at 4 K) of purified PSI trimers from *Synechocystis* PCC 6803 (top, vertically offset) and *Synechococcus* WH 7803 (bottom).

well-characterized PSI trimers from *Synechocystis* sp. strain PCC 6803 for comparison; see also Figure 1B of ref 8. The lowest electronic transition of Chl *a* in PSI of *Synechococcus* WH 7803 is at 700 nm and should therefore arise (at least in part) from the primary electron donor P700. Note that the width of this band is relatively small. In contrast, PSI from *Synechocystis* PCC 6803 shows apart from a small peak at 700 nm a much broader absorption at around 710 nm, which can be attributed to absorption from "red" Chls in this photosystem. These spectra suggest that PSI from *Synechococcus* WH 7803 contains much less red Chls than PSI of *Synechocystis* PCC 6803 and may not contain any red Chls at all.

The 77 K fluorescence emission spectra of isolated PSI trimers from *Synechococcus* WH 7803 and *Synechocystis* PCC 6803 are displayed in Figure 3. It is obvious that PSI of *Synechococcus* WH 7803 emits very little fluorescence at 77 K. The same was observed when performing 77 K temperature fluorescence experiments on whole cells (data not shown),

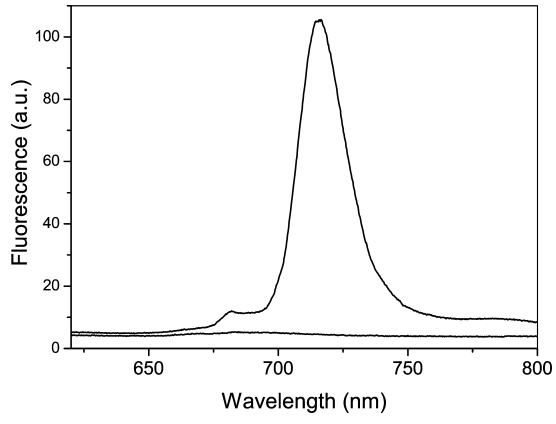

Figure 3. Fluorescence emission spectra (recorded at 77 K) with excitation at 440 nm of purified PSI trimers from *Synechocystis* PCC 6803 (top) and *Synechococcus* WH 7803 (bottom).

which was actually how *Synechococcus* WH 7803 was selected for this study. This is an unambiguous indication that these PSI complexes do not contain Chl molecules able to compete, at 77 K, with the trapping of the excitation energy by P700 and thus give rise to long-lived fluorescence. In this case indeed, excitation energy can rapidly be converted into potential chemical energy, and the fluorescence emission of PSI is photochemically quenched, also at 77 K, with a yield dependent on that of the primary electron-transfer reactions. Additionally, it may be concluded that the electronic absorption transition observed at 4 K at 700 nm in this PSI complex arises from P700 only.

Time-Resolved Emission at Room Temperature. Time-resolved fluorescence experiments with nonselective, 400 nm excitation were performed on isolated PSI trimers from *Synechococcus* WH 7803 at room temperature. Figure 4A

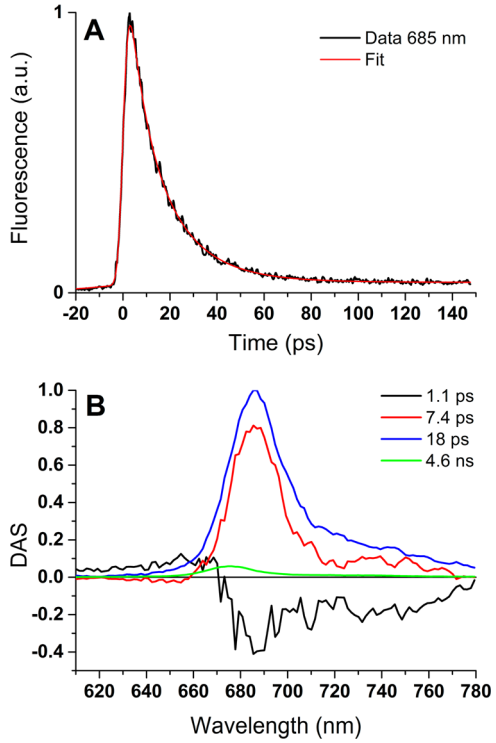

Figure 4. Emission of *Synechococcus* WH 7803 after 400 nm excitation (at RT). (A) The trace measured at 685 nm; the red line indicates the fit. (B) Estimated DAS.

shows a typical emission trace of these particles, measured at 685 nm. From a global fit of this trace together with the other 110 traces, four lifetimes and DAS were estimated, which are depicted in Figure 4B. The long-lived emission (4.6 ns, depicted in green) is attributed to the decay of a small fraction (~3.4%) of uncoupled Chl. The fastest phase (1.1 ps, black DAS) represents the transfer of energy from Q_x or other unrelaxed higher excited states to the Q_y states of all Chls in the PSI core complex. Note that this DAS is not conservative, indicating that some oscillator strength is gained, which can be explained by electronic relaxation from states that absorb in the Soret region. The 7.5 and 18 ps DAS represent the main decay phases. Both spectra peak at 685 nm, are of comparable magnitude and shape, but show significant differences in the red flank around 710−720 nm, where the 18 ps phase shows a larger amplitude. The spectra and kinetics of these decay phases

dx.doi.org/10.1021/jp401364a | J. Phys. Chem. B 2013, 117, 11176−11183

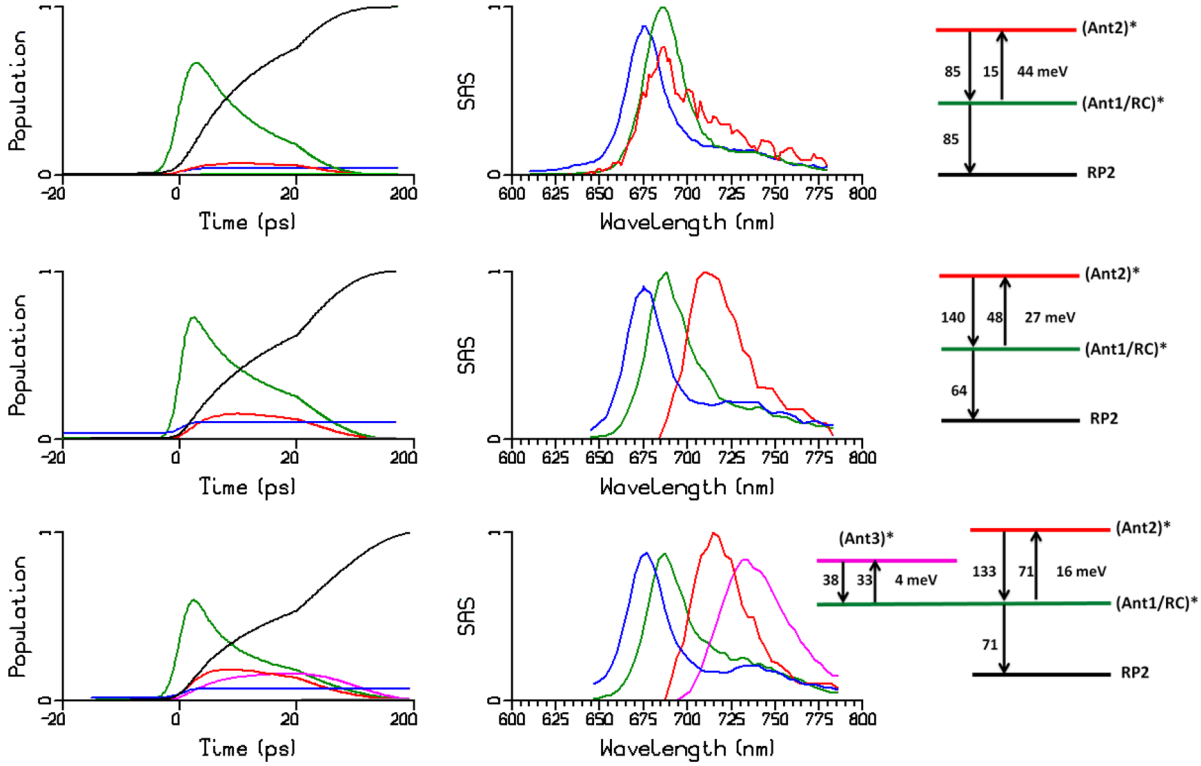

Figure 5. Compartmental models and target analysis results for PS1 cores at RT. From top to bottom: *Synechococcus* WH 7803, *Synechocystis* PCC 6803, and *Spirulina platensis*. From left to right: population profiles, estimated SAS, and kinetic schemes. The free Chl* (decaying with k_{fl}) and k_{fl} for excited states have been omitted for clarity. Estimated microscopic rate constants (to the left of each arrow) are in 1/(ns). Free-energy differences are indicated.

resemble those measured in *Chlamydomonas reinhardtii* by the same technique,[12] though the second phase is slightly longer in *Chlamydomonas* (~23 ps) than that in *Synechococcus* WH 7803 (~18 ps). Also in *Chlamydomonas*, the spectra of the ~8 and ~23 ps phases have slightly different shapes.[12] The small but significant differences in the shapes of these DAS can only be understood from a target analysis.

DISCUSSION

Target analysis. As they do not contain Chl absorbing at lower energy than P700, PSI from *Synechococcus* WH 7803 may be used to discriminate between the different models of excitation trapping in PSI. In Giera et al. (2010), the time-resolved emission data in *Chlamydomonas reinhardtii* were explained by the model (Ant/RC)* ↔ RP1 → RP2, in which RP1 represents the radical pair $A^+A_0^-$ and RP2 the stabilized radical pair $P700^+A_0^-$.[9] If this model were true, the spectra of the 8 and 23 ps decay phases would have to be identical, which is not the case. Giera et al. (2010) attributed the differences between the spectra to a further spectral equilibration of the excited states in about 7.5 ps.

A more elaborate model was put forward in ref 9, where transient absorption data were modeled as Ant* ↔ RC* ↔ RP1(a,b) → RP2(a,b), with the (a,b) expressing charge separation across both branches. In their model, the Ant* ↔ RC* equilibration takes ~1 ps. Because these authors assume that spectral equilibration is completed in 1 ps, the spectra of the 8 and 23 ps phases are also in this model expected to be identical, which is not the case.

Because of the different shapes of the 7.5 and 18 ps DAS in WH 7803, a successful target analysis using the above-mentioned models is not possible. In the following, we explore several possibilities for a target analysis in which these spectral differences are taken into account. The first (model 1) is a model in which there is an additional antenna state Ant2 that equilibrates slowly (e.g., in about 8 ps) with the bulk antenna, called Ant1 here, (Ant2)* ↔ (Ant1/RC)* ↔ RP1 → RP2. In this model, the DAS of the 8 ps phase would be a combination of the first charge separation reaction and further spectral equilibration. The second (model 2) is a model in which RP1 is supposed to be slighty emissive, (Ant/RC)* ↔ $(RP1)^{\delta}$* → RP2, which can be caused by a mixing of the charge-separated state of RP1 with (isoenergetic) excited states from surrounding Chl molecules. In this model, there is an ingrowth (negative signal) of $(RP1)^{\delta}$* in the ~8 ps phase and a decay, along with the other excited states, in the ~18 ps phase. The third (model 3) is a model in which the equilibration between the core antenna Chls (Ant*) and RC Chls (RC*) is on the order of 8 ps. Therefore, this model can be described by the scheme (Ant)* ↔ (RC)* ↔ RP1 → RP2, in which the first equilibrium (between Ant* and RC*) determines the 8 ps phase and is much slower than the subsequent process (equilibration between RC* and RP1). As in model 2, there will be an ingrowth (negative signal) of, in this case, RC* in the 8 ps phase and a decay of RC* along with Ant* in the 18 ps phase, thus explaining the different spectral shapes.

Model 1 Based on (Ant2)*. For a description of a minimal model with two emissive antenna states, we first lump the states (Ant1/RC)* and RP1 into one state because the emissions from (Ant1/RC)* and (Ant2)* are the only compartments that we can observe by time-resolved emission. Thus, a minimal model with two emissive states is given by (Ant2)* ↔ (Ant1/

dx.doi.org/10.1021/jp401364a | J. Phys. Chem. B 2013, 117, 11176−11183

RC)* → RP2. RP2 is equivalent to S2 of ref 12 and to RP2(a,b) of ref 9, while the (Ant/RC)* ↔ RP1 equilibria of ref 12 or the Ant*↔RC* ↔ RP1(a,b) equilibria of ref 9 are not yet included in the model. We thus assume that the (Ant/RC)* ↔ RP1 equilibrium is not rate-limiting and will return to this point later, where we will also address the ∼1 ps equilibration process.

We choose an equilibrium between two emitting compartments, the (Ant1/RC)* representing the equilibrated Chl of the bulk and RC (defined as the Chls in the center of the RC) and a slightly red-shifted Chl pool called (Ant2)*. Note that (Ant2)* does not necessarily have to be a "red Chl" (because that is defined as being red-shifted compared to P700); it represents Chls that are red-shifted compared to the bulk Chls (due to intrinsic inhomogeneous broadening) to account for the observed further spectral equilibration. The results from this target analysis are shown in the top row of Figure 5. The SAS of (Ant1/RC)* peaks at 685 nm (the dark green spectrum in Figure 5), while the SAS of free, uncoupled Chl peaks at 675 nm (the blue spectrum in Figure 5), typical for free Chl molecules.[26] The SAS of (Ant2)* also peaks at 685 nm (the red spectrum in Figure 5), but it possesses a broad red tail above 700 nm. From the population profiles, it is clear that its concentration is small, in accordance with a free energy of 44 meV above that of (Ant1/RC)*. To interpret the (Ant2)* compartment, the observed free-energy difference of 44 meV relative to that of (Ant1/RC)* must be decomposed. We estimate the energetic contribution from the difference between the average emission wavelength of the SAS, 696 and 705 nm for (Ant1/RC)* and (Ant2)*, respectively. This corresponds to 22 meV. The entropic free-energy difference thus equals 44 + 22 = 66 meV, which is equal to $k_BT \ln(N_1/N_2)$, with N_1 and N_2 as the number of pigments in the (Ant1/RC)* and (Ant2)* compartments. Using k_BT = 25 meV, we thus find N_1/N_2 = 13.4, which is consistent with N_1 and N_2 comprising ∼94 and ∼7 pigments, respectively.

The observed lifetimes of this kinetic scheme are 7.7 and 17.8 ps. The amplitude matrix (Table 1) demonstrates that

Table 1. Amplitude Matrix for the Different Lifetimes of *Synechococcus* WH 7803

compartment	(Ant2)*	(Ant1/RC)*	RP2	free Chl
excitation	0.024	0.976	0	0.038
7.7 ps	−0.192	0.562	−0.369	
17.8 ps	0.216	0.414	−0.628	
long-lived			0.997	
4.7 ns				0.038

(Ant2)* rises with 7.7 ps and decays with 17.8 ps. (Ant1/RC)* decays with both lifetimes, whereas RP2 rises with both lifetimes. Note that, eventually, the RP2 concentration in *Synechococcus* WH 7803 reaches 0.997, expressing that only 0.3% of the excitations is lost through fluorescence from the (Ant1/RC)* and (Ant2)* compartments.

Inspired by the success of this *Synechococcus* WH 7803 target analysis, we revisited the PS I core measurements of various cyanobacteria.[8] In that paper, it was demonstrated that one or two "red" (i.e., red-shifted compared to P700) antenna pools are present in the PS I core of all three species investigated *Synechocystis* PCC 6803, *Thermosynechococcus elongatus*, and *Spirulina platensis*. In the target analysis of ref 8, a single compartment was used for the "equilibrated antenna and RC". This compartment was in equilibrium with one or two red Chl compartments. Trapping was allowed from *all* compartments. Here, we allow for trapping only from the (Ant1/RC)* compartment. The results from target analyses of *Synechocystis* PCC 6803 and *Spirulina platensis* are shown in the second and third rows of Figure 5, respectively. Clearly, the SAS of (Ant2)* peaks at about 720 nm in both organisms, and the SAS of a third antenna component in *Spirulina* (Ant3)* peaks at 735 nm. An interesting result is that in contrast to ref 8, a trapping rate from the red Chl compartment(s) was no longer needed. Thus, this minimal target model can successfully describe energy-transfer and charge separation processes in PSI in *Synechococcus* WH 7803 and in other cyanobacteria.

We stress that the levels in Figure 5 are the levels of the free energies of the Chls in the various compartments. In case of *Synechococcus* WH 7803, the free-energy level of (Ant2)* is 44 meV *above* that of (Ant1/RC)*, while the energy level itself is most likely slightly lower. The entropy factor of the large number of bulk Chls in the (Ant1/RC)* compartment makes sure that the free energy of this state is considerably lower. In PSI of *Synechocystis* PCC 6803, the free-energy difference is reduced to 27 meV, which can be explained by the notion that (Ant2)* now represents real "red" Chls with lower energy levels. In PSI of *Spirulina*, the free-energy differences are even smaller.

An important motivation to include an (Ant2)* pool in all PSIs considered thus far is the low-temperature emission. By lowering the temperature, the relative free energy of red-shifted Chls gradually drops below that of the bulk Chl and of the RC. In *Synechococcus* WH 7803, the quantum yield of the emission appeared to be very low at 77 K (unlike, e.g., PSI from *Chlamydomonas reinhardtii* where red-shifted emission near 715 nm is present at 77 K).[14,15] In Figure 6, the shape of the tiny 77 K steady-state emission spectrum is redrawn (green spectrum) and compared with the (Ant2)* SAS (red spectrum; cf. Figure 5 top row). At 77 K, the (Ant2)* is expected to dominate the steady-state emission spectrum, which is indeed observed. The 670 nm peak in the green spectrum is attributed to free Chl*. A further cooling down to 5 K, however, resulted in emission peaking at 705 nm in *Synechococcus* WH 7803, in line with the proposed Ant2* state with free energy 44 meV above that of the bulk Chls (black spectrum in Figure 6).

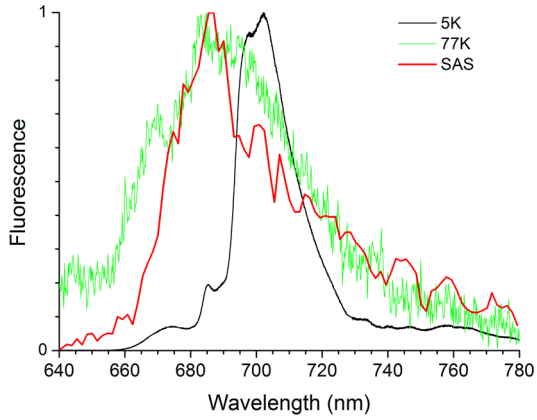

Figure 6. Comparison of estimated RT SAS (red) with shapes of the 77 K (green) and 5 K (black) steady-state emission spectra of purified PSI trimers of *Synechococcus* WH 7803.

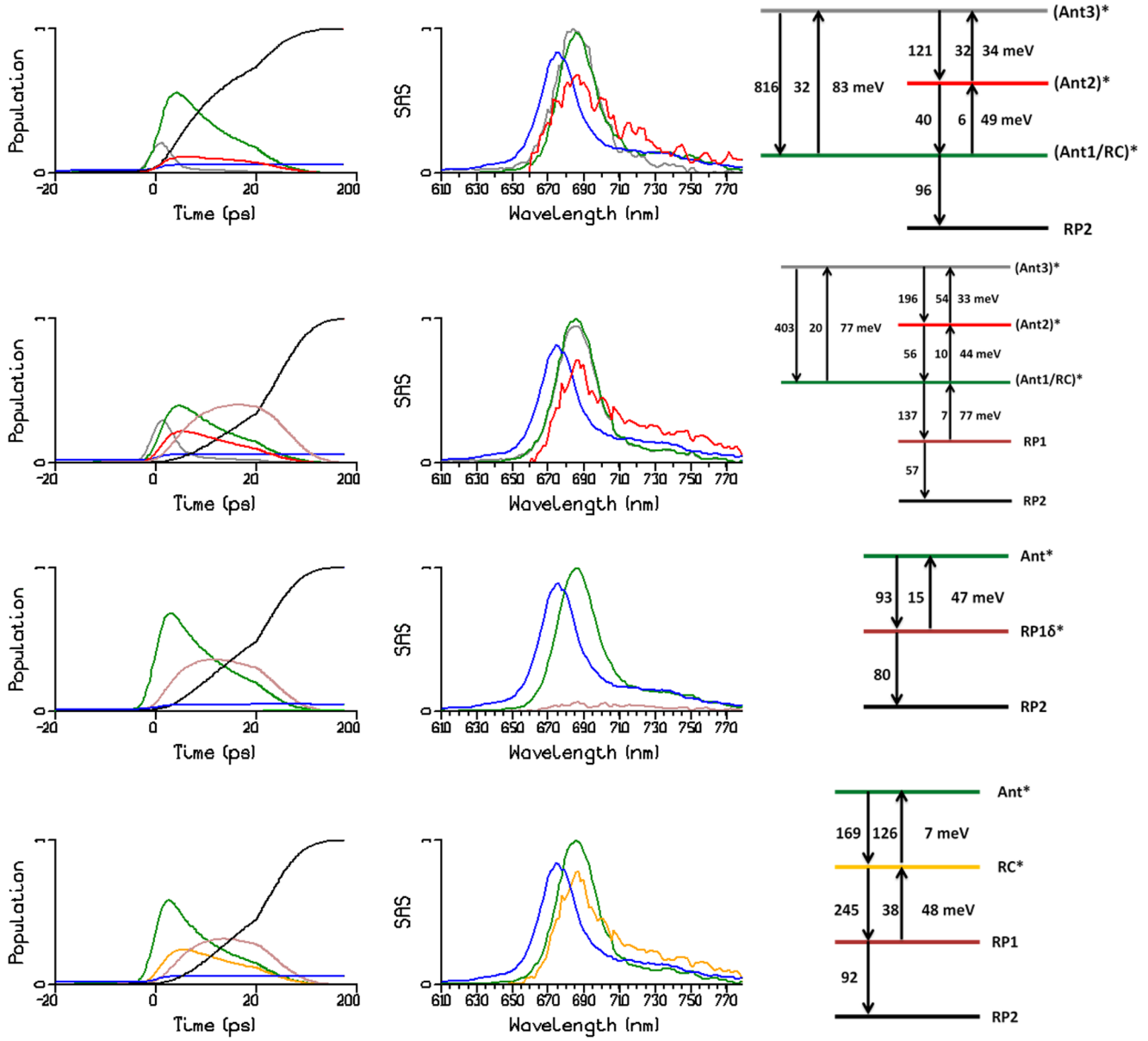

Figure 7. Alternative compartmental models for the PS1 core of *Synechococcus* WH 7803 at RT. The free Chl* (decaying with k_{fl}) and k_{fl} for emissive compartments have been omitted for clarity. Estimated microscopic rate constants (to the left of each arrow) are in 1/(ns). Free-energy differences are indicated. From left to right: population profiles, estimated SAS, and kinetic schemes. Top row: model 1 (Ant2)* ↔ (Ant1/RC)* → RP2 (see the top row of Figure 5) extended with (Ant3)*; second row: model 1 extended with (Ant3)* and RP1; third row: model 2 (Ant/RC)* ↔ RP1δ* → RP2; fourth row: model 3 (Ant)* ↔ (RC)* ↔ RP1 → RP2.

Extensions of Model 1 Based on (Ant2)*. We did investigate several alternative kinetic schemes for *Synechococcus* WH 7803, attempting to resolve the ∼1 ps equilibration process (black DAS in Figure 4B) and the (Ant1/RC)* ↔ RP1 equilibrium; see Figure 7. Equilibration components of ∼1 ps were also found in simulations; see, for example, refs 27−29. The top row of Figure 7 demonstrates that it is possible to add a third emissive compartment (Ant3)* that equilibrates with (Ant2)* and (Ant1/RC)* in ∼1 ps. Its SAS (in gray) is close to the SAS of (Ant/RC)* (in dark green), but it possesses more amplitude below 660 nm, as expected for unrelaxed states. The reconstructed DAS of this model, shown in Figure S1 (Supporting Information), closely resemble the DAS of Figure 4B, demonstrating that also this scheme extracts all information from the data.

In row two of Figure 7, an (Ant1/RC)* ↔ RP1 equilibrium was added. Adding this equilibrium resulted in the same quality of fit of the data. This target demonstrates that the data are consistent with a kinetic scheme that includes an (Ant1/RC)* ↔ RP1 equilibrium. The estimated rate constants and free energies are similar to those of the simple kinetic scheme depicted in the top rows of Figures 5 and 7. Note that the free energy of RP1 is estimated to be 77 meV below that of (Ant1/RC)*. The estimated rate constants (137 and 7/ns) are similar to those estimated in ref 9. From the amplitude matrix of this model, it follows that RP1 rises slowly (with time constants of 6 and 13 ps) and decays with 20 ps.

Model 2. Two different approaches (vide supra) have been investigated as well. The RP1δ* state assumes that RP1 is slightly emissive, which can be caused by a mixing of the

dx.doi.org/10.1021/jp401364a | J. Phys. Chem. B 2013, 117, 11176−11183

charge-separated state of RP1 with (isoenergetic) excited states from surrounding Chl molecules. The estimated RP1δ* SAS shows a broad spectrum that ranges from about 670 to 750 nm, which we attribute to coupling of the charge-separated state of RP1 with emissive states of nearby molecules. The area of this SAS is about 10% of the area of the (Ant/RC)* SAS. We conclude that a kinetic scheme (Ant/RC)* ↔ RP1δ* → RP2 (row three of Figure 7) cannot be ruled out, but we favor the scheme with an (Ant2)* pool because it also explains the low-temperature spectra and does not need to impose ultrafast (<1 ps) energy equilibration times, which are unrealistic given the spectral inhomogeneity of the antenna system (see also below).

Model 3. There is a long-standing debate[30,31] whether the charge separation or the energy transfer to the trap is the rate-limiting step. We also tested a kinetic scheme with relatively slow Ant* ↔ RC* equilibration (bottom row of Figure 7). Therefore, in this case, we have a scheme (Ant)* ↔ (RC)* ↔ RP1 → RP2. When the 7.5 ps DAS can be interpreted as a transfer-to-the-trap DAS, then the Ant* and RC* compartments equilibrate more slowly than the RC* and RP1 compartments. To estimate the Ant* and RC* equilibrium, we used the constraint that their SAS areas are equal. This resulted in a RC* SAS that was emitting more in the red (700−750 nm) than Ant* (compare the orange and dark green SAS in the bottom row of Figure 7). Following the same argument as above, the estimated free-energy difference of 7 meV is impossible to reconcile with the small difference in the SAS, in combination with the entropy advantage of Ant*, which is expected to be similar because the RC also contains six pigments. One would expect that the RC* free energy would be somewhat higher than that of Ant*, similar to the red Chl pools in Figure 5. Therefore, we consider this kinetic scheme unlikely.

In conclusion, we have re-established that equilibration between excited antenna Chls takes place on both fast (∼1 ps) and slow (∼8 ps) time scales. We note that at the excitation wavelength used in this study (400 nm), all Chls have about the same extinction coefficient, which means that, on average, each Chl has the same probability to absorb a photon after excitation. Therefore, if all Chls would have the same energy (absorption maximum), the system would be instantaneously fully spatially equilibrated. However, PSI contains several spectrally different pools of Chls with different Boltzmann factors. Therefore, what happens next is a preferential population of molecules with red-shifted excited states according to Boltzmann, resulting in further spectral equilibration. Our results suggest that this further equilibration to red-shifted states occurs for a large part in the peripheral antenna in about 8 ps. Time-resolved experiments at low temperature are needed to further unravel the equilibration between (Ant1)* and RC*.

Our minimal target model (Figure 5) can successfully describe energy-transfer and charge separation processes in PSI in *Synechococcus* WH 7803 and in other cyanobacteria. We have also successfully applied this model to *Chlamydomonas reinhardtii* (data not shown). This questions the models proposed in refs 9 and 12, which do not take into account a second antenna Chl compartment equilibrating on a ∼8 ps time scale. From our analysis, solely based on time-resolved emission, no further statements can be given on the involvement of an intermediary radical pair RP1, rising in about 8 ps and decaying in about 18 ps, because models with and without such a radical pair work equally well. The model, however, does give a straightforward explanation for the red-shifted low-temperature emission in the various cyanobacteria.

■ ASSOCIATED CONTENT

Supporting Information

DAS reconstructed from the target analysis. This information is available free of charge via the Internet at http://pubs.acs.org

■ AUTHOR INFORMATION

Corresponding Author

*E-mail: j.p.dekker@vu.nl.

Notes

The authors declare no competing financial interest.

■ ACKNOWLEDGMENTS

This project was carried out within the research programme of BioSolar Cells, cofinanced by the Dutch Ministry of Economic Affairs (I.H.M.v.S., J.J.S., R.v.G., and J.P.D.). I.H.M.v.S., B.R., and R.v.G. acknowledge financial support of the European Research Council (Advanced Grant Proposal 267333 (PHOTPROT) to R.v.G. and B.R.).

■ ABBREVIATIONS USED

Chl, chlorophyll; DAS, decay-associated spectrum; SAS, species-associated spectrum; PS I, photosystem I

■ REFERENCES

(1) Nelson, N.; Yocum, C. F. Structure and Function of Photosystems I and II. *Annu. Rev. Plant Biol.* **2006**, *57*, 521−565.

(2) Duval, J. C.; Thomas, J. C.; Choquet, Y. 77-K Fluorescence Quenching Induced by Reduction of Photosystem-I Primary Electron-Acceptors in a Cyanobacterium. *Biochim. Biophys. Acta* **1986**, *848* (3), 352−358.

(3) Karapetyan, N.; Schlodder, E.; Van Grondelle, R.; Dekker, J. P. The Long-Wavelength Chlorophylls of Photosystem I. In *Photosystem I: The Light-Driven, Plastocyanin:Ferredoxin Oxidoreductase*; Golbeck, J. H., Ed.; Springer: The Netherlands, 2006; pp 177−192.

(4) Wientjes, E.; van Stokkum, Ivo H. M.; van Amerongen, H.; Croce, R. The Role of the Individual Lhcas in Photosystem I Excitation Energy Trapping. *Biophys. J.* **2011**, *101* (3), 745−754.

(5) Slavov, C.; Ballottari, M.; Morosinotto, T.; Bassi, R.; Holzwarth, A. R. Trap-Limited Charge Separation Kinetics in Higher Plant Photosystem I Complexes. *Biophys. J.* **2008**, *94* (9), 3601−3612.

(6) Ihalainen, J. A.; van Stokkum, I. H. M.; Gibasiewicz, K.; Germano, M.; van Grondelle, R.; Dekker, J. P. Kinetics of Excitation Trapping in Intact Photosystem I of Chlamydomonas reinhardtii and Arabidopsis thaliana. *Biochim. Biophys. Acta* **2005**, *1706* (3), 267−275.

(7) Gobets, B.; van Grondelle, R. Energy Transfer and Trapping in Photosystem I. *Biochim. Biophys. Acta* **2001**, *1507* (1−3), 80−99.

(8) Gobets, B.; van Stokkum, I. H. M.; Rogner, M.; Kruip, J.; Schlodder, E.; Karapetyan, N. V.; Dekker, J. P.; van Grondelle, R. Time-Resolved Fluorescence Emission Measurements of Photosystem I Particles of Various Cyanobacteria: A Unified Compartmental Model. *Biophys. J.* **2001**, *81* (1), 407−424.

(9) Müller, M. G.; Slavov, C.; Luthra, R.; Redding, K. E.; Holzwarth, A. R. Independent Initiation of Primary Electron Transfer in the Two Branches of the Photosystem I Reaction Center. *Proc. Natl. Acad. Sci. U.S.A.* **2010**, *107* (9), 4123−4128.

(10) Müller, M. G.; Niklas, J.; Lubitz, W.; Holzwarth, A. R. Ultrafast Transient Absorption Studies on Photosystem I Reaction Centers from Chlamydomonas reinhardtii. 1. A New Interpretation of the Energy Trapping and Early Electron Transfer Steps in Photosystem I. *Biophys. J.* **2003**, *85* (6), 3899−3922.

(11) Holzwarth, A. R.; Müller, M. G.; Niklas, J.; Lubitz, W. Charge Recombination Fluorescence in Photosystem I Reaction Centers from

Chlamydomonas reinhardtii. *J. Phys. Chem. B* **2005**, *109* (12), 5903−5911.
(12) Giera, W.; Ramesh, V. M.; Webber, A. N.; van Stokkum, I.; van Grondelle, R.; Gibasiewicz, K. Effect of the P700 Pre-Oxidation and Point Mutations near A(0) on the Reversibility of the Primary Charge Separation in Photosystem I from Chlamydomonas Reinhardtii. *Biochim. Biophys. Acta* **2010**, *1797* (1), 106−112.
(13) Xu, W.; Chitnis, P.; Valieva, A.; van der Est, A.; Pushkar, Y. N.; Krzystyniak, M.; Teutloff, C.; Zech, S. G.; Bittl, R.; Stehlik, D.; Zybailov, B.; Shen, G.; Golbeck, J. H. Electron Transfer in Cyanobacterial Photosystem I: I. Physiological and Spectroscopic Characterization of Site-Directed Mutants in a Putative Electron Transfer Pathway from A0 through A1 to FX. *J. Biol. Chem.* **2003**, *278* (30), 27864−27875.
(14) Wollman, F. A.; Bennoun, P. A New Chlorophyll−Protein Complex Related to Photosystem-I in Chlamydomonas-reinhardii. *Biochim. Biophys. Acta* **1982**, *680* (3), 352−360.
(15) Tapie, P.; Choquet, Y.; Breton, J.; Delepelaire, P.; Wollman, F. A. Orientation of Photosystem-I Pigments — Investigation by Low-Temperature Linear Dichroism and Polarized Fluorescence Emission. *Biochim. Biophys. Acta* **1984**, *767* (1), 57−69.
(16) Wyman, M.; Gregory, R. P. F.; Carr, N. G. Novel Role for Phycoerythrin in a Marine Cyanobacterium, Synechococcus Strain dc2. *Science* **1985**, *230* (4727), 818−820.
(17) Schreiber, E. Die Reinkultur von Marinen Phytoplankton und deren Bedeutung für die Erforschung der Produktionsfähigkeit des Meerwassers. *Wiss. Meeresuntersuch., N.F.* **1927**, *10*, 1−34.
(18) Post, A. F.; Gal, A.; Ohad, I.; Milbauer, K. M.; Bullerjahn, G. S. Characterization of Light-Activated Reversible Phosphorylation of a Chlorophyll-a/B Antenna Apoprotein in the Photosynthetic Prokaryote Prochlorothrix-hollandica. *Biochim. Biophys. Acta* **1992**, *1100* (1), 75−82.
(19) Marquardt, J.; Rhiel, E. The Membrane-Intrinsic Light-Harvesting Complex of the Red Alga Galdieria sulphuraria (Formerly Cyanidium caldarium): Biochemical and Immunochemical Characterization. *Biochim. Biophys. Acta* **1997**, *1320* (2), 153−164.
(20) van Stokkum, I. H. M.; van Oort, B.; van Mourik, F.; Gobets, B.; van Amerongen, H. (Sub)-Picosecond Spectral Evolution of Fluorescence Studied with a Synchroscan Streak-Camera System and Target Analysis. In *Biophysical Techniques in Photosynthesis*; Aartsma, T. J., Matysik, J., Eds.; Springer: Dordrecht, The Netherlands, 2008; Vol. II, pp 223−240.
(21) van Stokkum, I. H. M.; Larsen, D. S.; van Grondelle, R. Global and Target Analysis of Time-Resolved Spectra. *Biochim. Biophys. Acta* **2004**, *1657*, 82−104.
(22) Holzwarth, A., Data analysis of time-resolved measurements. In *Biophysical Techniques in Photosynthesis*; Amesz, J., Hoff, A., Eds.; Kluwer Academic Press: Dordrecht, The Netherlands, 1996; pp 75−92.
(23) Mullen, K. M.; van Stokkum, I. H. M. The Variable Projection Algorithm in Time-Resolved Spectroscopy, Microscopy and Mass Spectrometry Applications. *Numer. Algorithms* **2009**, *51* (3), 319−340.
(24) Snellenburg, J. J.; Dekker, J. P.; van Grondelle, R.; van Stokkum, I. H. M. Functional Compartmental Modeling of the Photosystems in the Thylakoid Membrane at 77 K. *J. Phys. Chem. B* submitted to the same Festschrift.
(25) Nagle, J. F. Solving Complex Photocycle Kinetics — Theory and Direct Method. *Biophys. J.* **1991**, *59* (2), 476−487.
(26) Kwa, S. L. S.; Volker, S.; Tilly, N. T.; Vangrondelle, R.; Dekker, J. P. Polarized Site-Selection Spectroscopy of Chlorophyll-a in Detergent. *Photochem. Photobiol.* **1994**, *59* (2), 219−228.
(27) Brüggemann, B.; Sznee, K.; Novoderezhkin, V.; van Grondelle, R.; May, V. From Structure to Dynamics: Modeling Exciton Dynamics in the Photosynthetic Antenna PS1. *J. Phys. Chem. B* **2004**, *108* (35), 13536−13546.
(28) Renger, T.; Schlodder, E. Primary Photophysical Processes in Photosystem II: Bridging the Gap between Crystal Structure and Optical Spectra. *ChemPhysChem* **2010**, *11* (6), 1141−1153.
(29) Sener, M. K.; Park, S.; Lu, D. Y.; Damjanovic, A.; Ritz, T.; Fromme, P.; Schulten, K. Excitation Migration in Trimeric Cyanobacterial Photosystem I. *J. Chem. Phys.* **2004**, *120* (23), 11183−11195.
(30) van Grondelle, R.; Dekker, J. P.; Gillbro, T.; Sundström, V. Energy-Transfer and Trapping in Photosynthesis. *Biochim. Biophys. Acta* **1994**, *1187* (1), 1−65.
(31) van Grondelle, R.; Novoderezhkin, V. I.; Dekker, J. P. Modeling Light Harvesting and Primary Charge Separation in Photosystem I and Photosystem II. In *Photosynthesis in Silico: Understanding Complexity from Molecules to Ecosystems*; Laisk, A., Nedbal, L., Govindjee, Eds.; Springer: The Netherlands, 2009; pp 33−53.